Factors affecting the tensile strength of bituminous geomembrane seams

W. Francey[1] and R. K. Rowe[2]

[1] *PhD student, Queen's University, Kingston, Canada, E-mail: 15wjf@queensu.ca*
[2] *Professor, Queen's University, Kingston, Canada, E-mail: kerry.rowe@queensu.ca (corresponding author)*

ABSTRACT: The tensile shear strength, break location, and constant tensile load failure times are examined for seams made from one 4 mm-thick bituminous geomembrane (BGM) product, with corresponding observations specific to that material. In short-term tests, failure is observed within the sheet material once the seam strength exceeded 0.8 times that of the sheet material. The effects of seam thickness reduction and overlap width on seam strength are examined for two methods of seaming. Seams with a short-term strength meeting or exceeding 80% of the sheet strength are subjected to constant tensile loads between 18 and 55% of sheet ultimate strength and the time to failure is reported. The relationship between short-term seam strength and time to failure under sustained load and thickness reduction and squeeze-out is investigated. Constant tensile load testing is proposed as a construction quality assurance procedure to assess the degree of geotextile engagement of field seams.

1. INTRODUCTION

There is growing interest in the use of bituminous geomembranes (BGMs) as an alternative to widely used polyethylene geomembranes (GMBs) (Breul *et al.* 2008; Peggs 2008; Cunning *et al.* 2008; Addisi *et al.* 2013; Gourc and Delmas 2016; Clinton and Rowe 2017; Touze-Foltz and Farcas 2017; Daly *et al.* 2018; Samea and Abdelaal 2023). BGMs typically comprise a nonwoven geotextile impregnated with bitumen to provide a low hydraulic and low gas permeability material that retains a relatively high flexibility. The seaming technique for this material allows for faster installation and can be conducted using trained local labour rather than a specialized installation company (Mafra *et al.* 2008; Peggs 2008). High density polyethylene (HDPE) GMB seams are recognized as a weak point in the liners (Kavazanjian *et al.* 2017; Rowe and Shoaib 2017, 2018; Rowe and Francey 2018; Zhang *et al.* 2017; Francey and Rowe 2022, 2023a 2023b). Similarly, BGM seams are thought to be the weak point of the barrier system (Scheirs 2009).

Several papers have reported successful long-term applications of BGMs as hydraulic barriers. In one case study (Turley and Gautier 2004) two dams incorporating a 4.8 mm-thick BGM as an upstream barrier showed no reduction in watertightness after 25 years of operation. Touze-Foltz and Farcas (2017) reported that, after 30 years, there had been no change in the mechanical properties or flow rates through a BGM used as pond liner. Peggs (2008) reported that a BGM had performed adequately as an exposed landfill cover subjected to differential settlement and 20 years of exposure. Unfortunately, the magnitude of differential settlement was not discussed nor the condition of the seams. Similarly, Gourc and Delmas (2016) reported that a BGM used in a confined landfill cap and subjected to a relative elongation of 11% following differential settlement experienced a reduction in BGM burst strength. However, seam integrity or position within the settled zone was not discussed.

The papers discussed above all focused on the long-term tensile performance and/or water tightness of BGM sheet material and not the seams themselves, raising the question of how BGM seams may behave with time and what their likely failure mechanism may be in-field. Recent experience has highlighted the potential for failure of seams welded at elevated sheet temperatures. For example, Addis *et al.* (2013) examined a BGM seam failure at a co-disposal tailings storage facility in the Dominican Republic designed to contain potentially acid generating and metal leaching tailings. Upon identification of extensive seepage from one of the cells, three holes including a ~1.5 m × ~0.1 m large

tear, and open seams near the toe of the slope were identified. Partial to near complete seam failures were noted on panels primarily below the high-water level. These seams passed ultrasonic testing immediately after construction and were assumed to be free of air-voids within their 200 mm overlap. However, these seams could be pulled apart by hand and exhibited very little tensile shear strength. Two other tensile seam shear tests were conducted at elevated temperatures, and a significant reduction in the maximum seam tensile strength was observed.

The paucity of published data on BGM performance, indication that seams may have low strength after passing ultrasonic testing (Addis *et al*. 2013), and seams generally accepted as a weak point in the barrier system (Scheirs 2009), has prompted this examination of the suitability of currently employed qualitative assessment and destructive testing construction quality assurance (QCA) procedures. The work presented herein aims to examine a minimum seam shear strength value for field-seamed BGMs in accordance with ASTM D7056-07. Furthermore, the seam break characteristics and constant load failure time will also be examined with respect to seam tensile shear strength. The objectives of this study are to: (1) examine the suitability of the manufacturer recommended 200 mm overlap width for seams based on seam strength and break location criteria, (2) identify a 'weld factor' that can be used as a criteria for assessment of seams with suitable strength and break location, and (3) explore any relationship that may exist between thickness reduction and squeeze-out on BGM seam tensile performance.

2. MATERIAL AND METHODS

The BGM material examined (TERANAP 431-4M) was a 4 mm (nominal) thickness BGM containing a glass fleece layer. Tensile strength was measured in accordance with ASTM D7275-07. The machine direction ultimate tensile strength was 27.1 ± 1.4 kN/m. The cross-machine direction (XD) value was 21.8 ± 1.0 kN/m. The XD is considered the most relevant strength for comparing BGM seam to sheet. This is because seamed panels of BGM are generally oriented parallel to the machine direction, meaning shear and tensile loading on a BGM seam will predominately engage the material in the XD. As a result, all seamed samples examined herein are XD oriented, allowing for a direct comparison between the observed XD seam and sheet strength values.

2.1. Hand-torch seaming
Twelve hand-torch BGM seam specimens were created in the laboratory at 21°C using a hand-held Bernzomatic propane torch often used in-field for the seaming of patches or chamfering of seam edges. Desired overlap widths were marked on the sheet prior to welding. Both the top and bottom sheet were heated until the bitumen coat across the area to be seamed was melted and bubbling. The heated sheets were then placed on top of each other, and pressure was applied according to a predetermined method for each seam group. One seam group was subjected to a 5 kPa static compressive stress for 1 min. Other seams were created using

a hand roller immediately post-heating and placement. Two different levels of dynamic hand-roller seaming stress were employed. Once seamed, specimens were left to cool at room temperature for 24 h. Thickness measurements were made prior to tensile testing 50 mm × 400 mm BGM strips.

2.2. Field-torch seaming
All field torch seaming was conducted outdoors at 15°C ambient temperatures on a compacted well-graded gravel pad by an experienced technician. The BGM panels were overlapped by 200 mm along their machine direction, the packaging strip along leading panel edges was removed, and the overlap sections of BGM were heated using a single nozzle propane torch and subsequently seamed together with a 10 kg steel roller. The width over which the bitumen was melted to form the seam varied from 63 mm to 205 mm to provide specimens with different levels of overlap. Following seaming, the seams were left to cool, in situ, for approximately 1 h. After cooling, 1.0 m by 1.0 m BGM samples were carefully packaged and transported to laboratory for storage at 21 ± 2°C. After more than 24 h acclimatization to laboratory conditions, twelve tensile shear strength and twelve constant load tensile rupture specimens were cut from six field-torch seams using a stainless-steel blade. Care was taken to avoid irregularities or notching along sample edges.

2.3. Tensile shear strength testing
Twelve tensile shear strength tests were conducted in accordance with ASTM D7056-07 on specimens from six different field seams. Seamed specimens were 50 mm wide and had a minimum length 200 mm greater than the seam overlap (i.e. 400 mm-long for a 200 mm seam). Seamed specimens were gripped 50 mm from each leading edge of the overlap, resulting in an initial grip separation 100 mm greater than the corresponding seam overlap width. The shear strength tests were performed at a 50 mm/min grip separation rate until rupture. After rupture, the break location of the seam was recorded as either having occurred within the sheet material adjacent to the seam, or within the seam itself.

2.4. Constant tensile load testing
Twelve constant tensile load tests were conducted using a modified ASTM D5262-07 procedure. Specimens were 200 mm-wide by 400 mm-long to allow 50 mm of sheet material (after clamping) on either end of the 200 mm overlap BGM seam, providing a 300 mm gauge length. Selected load increments (of ~10%) were based on the ASTM D7275-07 XD tensile strength, corresponding to 18.4% (4 kN/m), 27.5% (6 kN/m), 36.7% (8 kN/m), 45.9% (10 kN/m), and 55% (12 kN/m) of the material ultimate strength, with the minimum and maximum loads selected based on test duration limitations and the load limit of the testing grips. Loading rate was 50 mm/min (i.e. rate at which load was applied to reach constant load) at a temperature of 21 ± 2°C. Both time until rupture and grip separation at rupture were recorded.

2.5. Seam thickness reduction

Seam thickness reduction was measured using calipers as this method was thought to be more easily implemented for in-field use. Seam thickness reduction is defined as the sum of the thicknesses of both the top and bottom GMB, or combined thickness of the two sheets to be seamed, minus the thickness of the seam (Equation 1) (Scheirs 2009).

$$t_r = (t_t + t_b) - t_s \qquad (1)$$

where t_r is the seam thickness reduction, t_s is the thickness of the seam, and t_t and t_b are the thickness of the top and bottom sheet, respectively. An average of six measurements, three on each side of the specimen to be tested, were used as the representative thickness reduction value. Measurements were taken 25 mm from both ends of the overlapped section of the seam as well as the overlap midpoint (for a total of three per side). Sheet thickness was also measured using caliper to assess conformance with the manufacturer specified average thickness. An average of ten thickness measurement using calipers (4.1 ± 0.04 mm thickness) showed good agreement with the manufacturer specified average thickness of 4.1 mm.

3. RESULTS AND DISCUSSION

3.1. Tensile strength of hand-torch and field-torch seams

Seam tensile shear strength was examined for 24 seam specimens using two different welding torches and a seam overlap width range from 50 mm to 200 mm. Five replicate tests were conducted for a 200 mm wide field torch and 10 kg roller (Table 1) to evaluate seam preparation repeatability. The average width of these 200 mm nominal seams was 202.6 ± 2.4 mm with a 1% coefficient of variation, which is considered very good for field welded seams. The seam break strength was 20.0 ± 0.7 kN/m with a coefficient of variation of 3%. Similarly, the weld factor (the ratio between a seam break strength and that of the sheet material) averaged 0.92 ± 0.03 with a coefficient of variation of 3.7%. All three measures highlight the repeatability of the seams that were produced in terms of the seam break strength.

Both field-torch and hand-torch seamed specimens displayed increased tensile strength with increased seam overlap width (Table 1). Nevertheless, despite the use of two different torches and four different means of applying pressure, the results were very consistent for three of the four means of compression. Excluding the 5 kPa static load compression results discussed below, the seven 200 mm wide seams exhibited an average weld factor of 0.93 with coefficient of variation of 3%. Similarly, the 150 mm wide seams exhibited an average weld factor of 0.93 and a coefficient of variation of 5%. This provides additional evidence regarding the repeatability of the data.

Hand-torch seams created with a low 5 kPa static load seaming stress had a thickness reduction averaging 0.15 mm. The peak seam strength increased monotonically with increasing seam overlap width with a corresponding increase in weld factor from 0.55 to 0.76 as the seamed width increased from 50 to 200 mm. It is apparent that the

Table 1. Seam parameters and resulting tensile shear strength for all seams examined in accordance with ASTM D7056-07

Seaming method	Seaming compression	Seam overlap width (mm)	Thickness reduction (mm)	Peak seam strength (kN/m)	Weld factor	Break location
Hand torch	5 kPa: Static load	50	0.2 ± 0.16	12.0	0.55	
		100	0.2 ± 0.08	14.4	0.66	
		150	0.1 ± 0.07	15.5	0.71	Seam
		200	0.1 ± 0.09	16.6	0.76	
Hand torch	Hand roller: Moderate	50	0.7 ± 0.15	13.9	0.64	
		100	0.9 ± 0.33	17.5	0.80	Seam
		150	0.9 ± 0.30	19.3	0.89	
		200	0.8 ± 0.28	20.6	0.94	Sheet
Hand torch	Hand roller: High	50	2.1 ± 0.09	17.0	0.78	Seam
		100	1.4 ± 0.11	20.7	0.95	
		150	1.5 ± 0.39	21.4	0.98	Sheet
		200	1.4 ± 0.10	21.0	0.96	
Field torch	Field roller	63	0.3 ± 0.13	14.8	0.68	Seam
		71	0.8 ± 0.32	19.4	0.89	
		110	0.2 ± 0.10	19.5	0.89	
		115	0.8 ± 0.50	19.4	0.89	
		144	0.2 ± 0.04	20.2	0.93	
		174	0.5 ± 0.16	20.0	0.92	
		188	0.2 ± 0.09	20.6	0.94	Sheet
		200	0.1 ± 0.07	19.5	0.89	
		200	0.2 ± 0.14	20.4	0.94	
		204	0.4 ± 0.25	19.2	0.88	
		204	0.7 ± 0.28	20.2	0.93	
		205	0.4 ± 0.17	20.9	0.96	

Both hand-torch and field-torch seams that displayed a weld factor >0.8 (with one exception effectively at this limit) experienced failure within the sheet material rather than within the seam

5 kPa static load was not sufficient to obtain good seams. Using the same torch and increasing the pressure and thickness reduction to 0.83 mm, the weld factor increased monotonically from 0.64 to 0.94 with increasing seam width from 50 to 200 mm. Even higher pressures increased the thickness reduction to an average of 1.6 mm, in this case even the 50 mm seam had a weld factor of 0.78 with the other three seam widths of 100, 150 and 200 mm all having a weld factor between 0.95 and 0.98, indicating a high-quality seam. Thus, in summary, and for a given overlap width, the hand-torch seams exhibited increased tensile strength with increasing thickness reduction within the seam (Figure 1a) and the greater the thickness reduction of a seam the less overlap width was necessary to achieve near sheet strength values.

Of the 12 field torch seams, only the narrowest (63 mm wide) seam had an unacceptable weld factor of 0.68 with a thickness reduction of 0.3 mm. All the larger overlaps, between 71 and 205 mm, had weld factors between 0.88 and 0.96, meeting the typical requirement of 0.8, and all failed in the sheet and not in the seam (Figure 1b). The generally good performance of the field roller seams is attributed to both the increased heat during seaming for field-torch seams, and/or the different seaming stress induced by the 10 kg steel field-roller, effectively creating stronger seams (relative to hand-torch seams) for small, welded areas. Once a seam had reached near sheet material strengths, and the break location shifted from the seam to the sheet, no further increase in seam strength was observed following further increases in overlap width or thickness reduction.

No seams exhibited a strength value greater than the ASTM D7275-07 sheet material strength. The average weld factor for all field seams that failed in the sheet was 0.91 with a standard deviation of 0.03. The failure locations for seams that failed in the sheet shifted from the center of the sample (the location of failure for ASTM D7275-07 sheet specimens) to areas closer to the grips, as the much thicker seam itself occupied the middle portion of the test specimen. Moreover, the ASTM D7275-07 sheet samples and ASTM D7056-07 seam samples have different dimensions, suggesting the geometry of seam tensile shear specimens may have influenced peak strengths and failure position relative to ASTM D7275-07 sheet specimens. To test this hypothesis, four 50 mm by 300 mm sheet specimens (i.e. same dimensions as the seams) were tested and yielded an average ultimate strength of 20.3 ± 0.6 kN/m, a value close to the average ultimate strength of seams that experienced failure within the sheet (20.1 ± 0.7 kN/m). This supports the hypothesis that the difference in ultimate strength between ASTM D7056-07 seams specimens and ASTM D7275-07 sheet specimens was primarily the result of differences in specimen geometry. However, in the following, the seam weld factor was calculated by dividing the ultimate strength of the seam by the sheet ultimate strength, obtained following ASTM D7275-07, since this is what is likely used in the field.

The highest observed seam strength value for a seam that experienced failure in the seam was 17.5 kN/m (100 mm overlap, hand roller moderate seam), while the lowest recorded strength for a seam that experienced failure within the sheet was 19.2 kN/m (200 mm overlap, field-torch seam). Normalizing each of these values to the sheet material strength resulted in a weld factor of 0.80 and 0.88, respectively. As per manufacturer guidelines, a 0.8 weld factor is often employed as a lower limit for acceptance of BGM seam based on their ASTM D7056-07 tensile strength. Given the maximum recorded strength for seams with failure in seam is essentially at this limit, and that all seams that observed failure in the sheet were in excess of the 0.8 weld factor, this criteria appears to be a reasonable lower limit to accept seams based on seam break location following short-term tensile shear testing.

Another manufacturer's installation guidelines recommended a 200 mm seam overlap width (Turley and Gautier 2004; Breul *et al*. 2008). All 200 mm-overlap field-torch seams experienced both a weld factor >0.8 and failure within the sheet material. Thus, this recommended
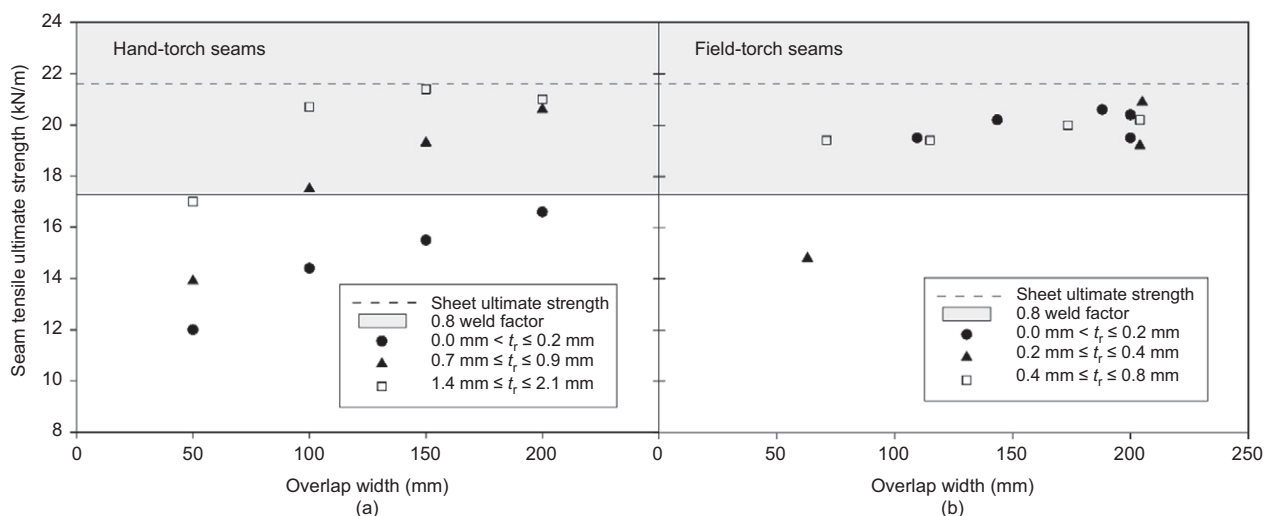

Figure 1. Seam tensile ultimate strength for different overlap width and thickness reduction for (a) hand-torch seams, and (b) field-torch seams

seam overlap width appears reasonable for field torch seams. In contrast however, a 200 mm overlap hand-torch seam with a thickness reduction of 0.1 mm experienced failure within the seam, indicating that simply specifying a 200 mm overlap is not sufficient to ensure adequate strength and break locations for hand torch seams in the field. Thus, a thickness reduction ≥0.2 mm should be achieved to provide redundancy in the event poor heating or seaming stress is applied during seaming of a 200 mm overlap seam.

3.2. Constant tensile load performance

Constant tensile load tests were initially performed on two different 200 mm overlap field-torch BGM seams at constant loads of 18.4% (4 kN/m), 27.5% (6 kN/m), 36.7% (8 kN/m), 45.9% (10 kN/m), and 55% (12 kN/m) the sheet material ultimate strength. All specimens tested in a constant tensile load test, despite having passed the 0.8 weld factor and break location criteria in a tensile shear test, experienced failure within the seam rather than within the sheet material. This suggests that although tensile shear testing can provide an immediate indication of bond strength, constant tensile load testing may provide a better indication of seam strength with time and that BGM seams may be susceptible to long-term tensile loads perpendicular to the direction of the seam. Failure times ranged from 0.03 days (0.1 mm thickness reduction at 45.9% sheet ultimate strength) to 4.55 days (0.4 mm thickness reduction at 27.5% sheet ultimate strength), with a notable difference in failure time between the two seams at a given load (Table 2). Plotting a power function to the time until rupture data, as recommended by ASTM D5262-07, gave

$$\chi = 20.61 \times t_{NF}^{(-0.211)} \qquad (2a)$$

or inverted

$$t_{NF} = \exp\left[\frac{-\ln(\chi) - 3.03}{0.211}\right] \qquad (2b)$$

and $R^2 = 0.95$ for the seams with thickness reduction $t_r = 0.1$ mm, and

$$\chi = 41.10 \times t_{NF}^{(-0.266)} \qquad (3a)$$

or inverted

$$t_{NF} = \exp\left[\frac{-\ln(\chi) - 3.72}{0.266}\right] \qquad (3b)$$

where $R^2 = 0.98$ for the seams with thickness reduction $t_r = 0.4$ mm, $\chi = T/T_{ult}$ (%) is the applied load, T, as a percent of the cross-machine direction tensile ultimate strength of the sheet, T_{ult}, and t_{NF} is the time until rupture in days. Interpolating failure times using the fitted power function for the various loads yielded an order of magnitude difference in failure time between the two seams examined (Figure 2). Given that BGM seams rely on bitumen within the overlap to provide tensile strength to the seam, one would suspect BGM seams to be susceptible to sustained tensile loads given the viscous nature of bitumen. Due to the observed difference between seams, a mechanism other than just the strength of the bitumen must have contributed to the observed difference in performance between seams, one which may be detected by monitoring a seams thickness reduction.

Strain at rupture was calculated using grip separation at the point of seam rupture and an initial gauge length of 300 mm. Strain at rupture for both seams was found to decrease with decreasing applied load, with the minimum strain at rupture being ~10–13% and ~25–33% for the $t_r = 0.1$ mm and $t_r = 0.4$ mm seams (Table 2; upper half), respectively. For a given applied load, $t_r = 0.1$ mm seams displayed an ~35% reduction in the strain at break compared with the $t_r = 0.4$ mm seams, suggesting the mechanism contributing to faster failure times may also have contributed to a lower strain at break for a given load.

The foregoing results provide insight regarding thickness reductions of 0.1 mm (squeeze-out 0 mm) and 0.4 mm (squeeze-out 6–10 mm). One manufacturer recommends a minimum squeeze-out of 6 mm (Mafra *et al*. 2008). To examine the effect of squeeze out, four additional seams having (squeeze-out; t_r) of (0 mm;

Table 2. Constant tensile load failure times and strain at rupture for two different thickness reduction seams tested at loads ranging from 4–12 kN/m

Thickness reduction (mm)		0.1 ± 0.06	0.4 ± 0.18	0.1 ± 0.06	0.4 ± 0.18	0.1 ± 0.06	0.4 ± 0.18
Load (kN/m)	% Sheet UTS	Time to rupture (days)		Strain at rupture (%)		Squeeze out (mm)	
4	18.3	1.64	—	~10–13[a]	—	0	—
6	27.5	0.3	4.55	16	~25–33[a]	0	6–10
8	36.7	0.04	1.57	26	~37–43[a]	0	6–10
10	45.9	0.03	0.57	30	47	0–5	6–10
12	55	—	0.38	—	58	—	6–10

Load (kN/m)	% Sheet UTS	Thickness reduction (mm)				
10	45.9	0.1 ± 0.07	0.2 ± 0.14	0.4 ± 0.17	0.6 ± 0.33	0.7 ± 0.28
Squeeze out (mm)		0–5	0	6–10	20–27	25–55
Time to rupture (days)		0.03	0.04	0.57–0.63	0.41	0.45
Strain at rupture (%)		30	37	45–47	42	44

[a]Specimen strain at rupture estimated due to lower measurement frequency at longer testing durations.

$t_r = 0.2$ mm), (6 mm; $t_r = 0.4$ mm), and (20–55 mm; $t_r = 0.6$–0.7 mm) were examined (Table 2; lower half). All these seams had a weld factor >0.8 and tensile shear failure in the sheet. Like the previous $t_r = 0.1$ mm and $t_r = 0.4$ mm seams, a sustained constant load test resulted in failure within the seam rather than the sheet, with an order of magnitude lower seam failure time for seams with thickness reduction ≤0.2 mm compared to seams with thickness reduction >0.2 mm (Figure 3). However, the 0.6–0.7 mm thickness reduction seams (with squeeze-out beads ranging from 20–55 mm), exhibited an average 28% reduction in seam rupture time when compared with the 0.4 mm seams. Thus, both too little and too much squeeze-out may indicate faster constant tensile load rupture in BGM seams. Greater thickness reduction

resulted from greater bitumen loss within the seam interface and greater squeeze-out. It appears that for better longer-term constant tensile load rupture resistance there is an optimum range of bitumen thickness between the geotextile layers with too much ($t_r \leq 0.2$ mm) minimizing the beneficial interaction between the geotextile and bitumen and too little ($t_r \geq 0.6$ mm), also reducing the effectiveness of the interaction although to a lesser extent than too much bitumen. Thus, the optimum condition for this particular BGM appears to be $0.2 < t_r < 0.6$ mm with an optimal thickness reduction of ∼0.4 mm and squeeze out of ≥6 mm.

3.3. Evidence of geotextile engagement

The failure surface morphology of both tensile shear and constant tensile load specimens were examined following rupture and a notable difference was observed for seams that failed within the sheet versus those that failed within the seam. In the event seam failure occurred within the sheet (for tensile shear specimens), a small portion of the overlap within that seam was generally separated during testing and exposed a portion of the geotextile core. This was also noted for constant load specimens, where the 0.4 mm thickness reduction seam's failure surfaces showed a rough surface texture and an exposed geotextile core following rupture. This morphology was absent on the 0.1 mm thickness reduction seams for both tensile shear specimens and the constant load specimens, and instead a smooth bitumen surface and no exposed geotextile core was present after rupture (Figure 4).

Seams with a thickness reduction ∼0.4 mm generally exhibited exposed geotextile core failure surfaces, and for the constant load tensile tests, this difference occurred in conjunction with an order of magnitude higher failure time and greater strains at rupture. It is hypothesized that heating of the bitumen impregnated within the geotextile, or the application of stress forcing the softened bitumen into the
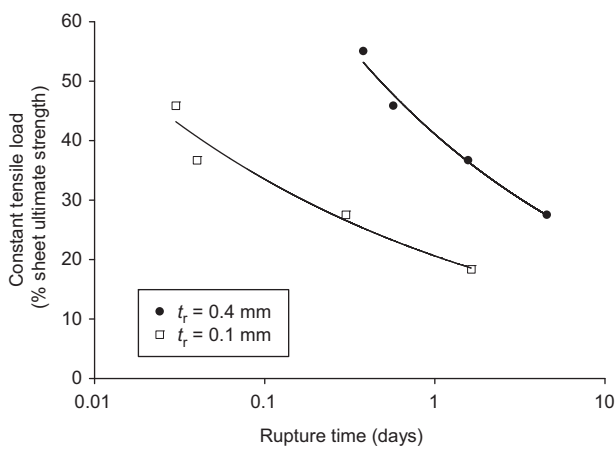
Figure 2. Fitted power functions on constant tensile load rupture data for the 0.1 mm and 0.4 mm thickness reduction BGM seams. Interpolating failure times between these curves for the load range examined yielded an order of magnitude shorter failure time for the 0.1 mm thickness reduction seam compared to the 0.4 mm thickness reduction seam
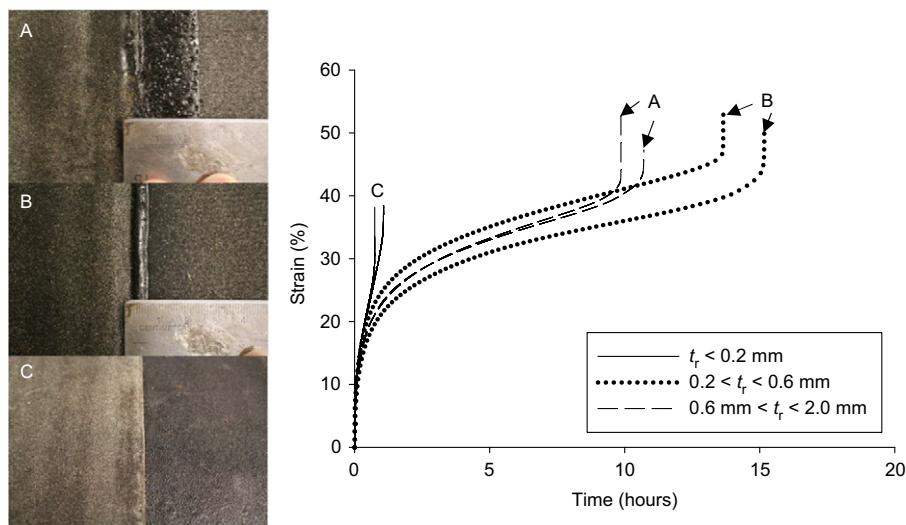
Figure 3. Strain vs time for the six constant tensile load tests conducted at 10 kN/m (45.9% material ultimate strength load). Time until rupture was an order of magnitude greater for seams with ≥6 mm squeeze-out and >0.2 mm thickness reduction. Seams with squeeze-out amounts ≥20 mm (seam group A) experienced a 28% reduction in seam failure time compared with 6–10 mm squeeze-out seams (seam group B), although failure times were still an order of magnitude greater than <6 mm squeeze-out seams (seam group C)

Figure 4. **Constant tensile load failure surfaces of the 0.1 mm and 0.4 mm thickness reduction BGM seams. In the 0.4 mm thickness reduction case, a rough exposed geotextile surface was present after testing, with fibers oriented in the direction of applied load. This was absent in the 0.1 mm thickness reduction seam. Given the order of magnitude difference in failure time between these seams, these failure surfaces suggest geotextile engagement played an important roll in seam failure time**

geotextile pores, resulted in greater geotextile engagement and longer failure times for the higher thickness reduction seams. Geotextile engagement was evident based on the exposed geotextile core and orientation and elongation of geotextile fibers along the axis of applied stress. The two most likely mechanisms contributing to the increased constant tensile load strength of seams following geotextile engagement are: (1) that increased melt depth, or softening of the bitumen within the geotextile core, as well as displacement of bitumen into any potential air voids present within the geotextile, increased the number of fibers engaged during tensile testing, and/or (2) that more intimate contact between the two sheets increased the interface friction of the seam interface, increasing seam performance when subjected to tensile stress. These two factors are not mutually exclusive and may have both contributed to the relative difference in performance between seams. Furthermore, there is the potential for the geotextile cores (of both sheets in the overlap) to become heat tacked to each other, as heat tacking is a common method for sealing geotextile overlaps in the field. However, during heating the geotextile cores are not exposed as they are when heat tacking geotextile seams, effectively limiting the heat they're exposed to and their degree of intimate contact when forced together. Thus, this factor was expected to have played a limited role in the observed difference in seam constant tensile load performance.

3.4. Tensile shear vs constant tensile load testing

The proceeding sections demonstrated that one can obtain a good short-term tensile break strength with BGM seams (Table 1) but that a sustained load of only 30% of the short-term break load was sufficient to cause seam failure (Figure 2). This implies that it may be necessary to limit the tensile force in BGMs, especially at seams, and BGM seam long-term performance may be better assessed using a constant tensile load testing. Although short-term tensile shear testing of BGM seams is still needed for an immediate assessment of seam short-term strength in the field, as poor seaming may lead to immediate rupture following installation.

Considering the results presented in the three preceding subsections, it can be concluded that tensile shear testing may be useful for excluding some unsatisfactory BGM seams but is not sufficient for concluding that a seam has adequate long-term integrity when subjected to sustained tensile stress perpendicular to the seam direction. Seams with little or no bitumen squeeze-out and/or low thickness reduction are less likely to have adequate geotextile engagement. When a CQA engineer suspects inadequate engagement of the geotextile in the seam, they can conduct a constant tensile load test and examine the resulting failure surfaces of the BGM seam. Ideally both the upper and lower sheet materials being seamed should exhibit some degree of geotextile engagement. If a smooth bitumen surface is present, and no geotextile core exposed, then the seam is likely not adequate due to inadequate seaming stress and/or applied heat. Adding this testing metric to existing CQA procedures, such as tensile shear and ultrasonic testing, will provide further confidence of seam long-term integrity.

4. GENERAL DISCUSSION AND PRACTICAL APPLICATIONS

4.1. Service life of seams subjected to sustained tensile strains

The tests conducted in this paper have focused on the unconfined response and rupture times of seams subjected to constant tensile loads. The BGM seam failures observed in this study are similar to those observed in field applications (e.g. Addis *et al.* 2013). Based on Equations (2b) and (3b), preliminary estimates of the time to failure of the seam (rupture) at various ratios of the tensile load to the ultimate tensile load of the sheet, χ, for the two values of thickness reduction (0.1 mm, 0.4 mm) equations predict at $\chi = 2\%$ a failure time of (180, 240) years, $\chi = 3\%$ of (25, 52) years, $\chi = 4\%$ of (7, 18) years, $\chi = 5\%$ of (2, 8) years, $\chi = 6\%$ of (1, 4) years, and $\chi = 7\%$ of (0.5, 2) years. While there is uncertainty associated with extrapolation, these preliminary estimates identify tensile stress as a potential problem for BGM seams. Based on the relationship established for this particular BGM, to get a seam service life greater than 50 years with

$t_r = 0.4$ mm and $t_r = 0.1$ mm, the sustained tensile stresses must be less than 3% and 2.6% of the ultimate tensile strength of the sheet at room temperature, respectively. These times may well be accelerated at elevated temperatures. While these results must be regarded as preliminary, they indicate the need for more investigation into the effects of even small tensile forces (e.g. from differential settlement and covers) on long-term BGM seam performance.

The 71 mm, 110 mm, 115 mm, and 144 mm overlap field seams (Table 2) were less than the specified seam overlap width retention criteria of 75% (i.e. minimum of 150 mm overlap retained for a 200 mm overlap seam) employed in the case study by Turley and Gautier (2004), yet they still exhibited a short-term strength weld factor >0.8. This supports the idea that a 200 mm overlap specification provides redundancy regarding a seam's short-term tensile strength, and that seams with less than 200 mm overlap may still exhibit desirable short-term strength and break locations. However, in the Addis *et al.* (2013) case study, 200 mm seam overlap was employed with seams noted as having passed ultrasonic testing (indicating continuity along the 200 mm overlap), yet they still exhibited poor strength values and separated after a few months of operation. At 20°C this could occur in a few months (assumed ~4 months) for $t_r \sim 0.4$ mm at 11–12% of the ultimate tensile strength and for $t_r \sim 0.1$ mm at about 7–8% of the ultimate tensile strength. This difference in behavior suggests that despite a continuous 200 mm overlap that another factor (potentially lack of geotextile engagement) in addition to high sheet temperature was contributing to these reported differences in seam strength. Thus, for the geomembrane tested, simply meeting the 200 mm overlap specification is not adequate for ensuring

the long-term performance of a BGM seam and tensile testing is necessitated to identify faulty seams.
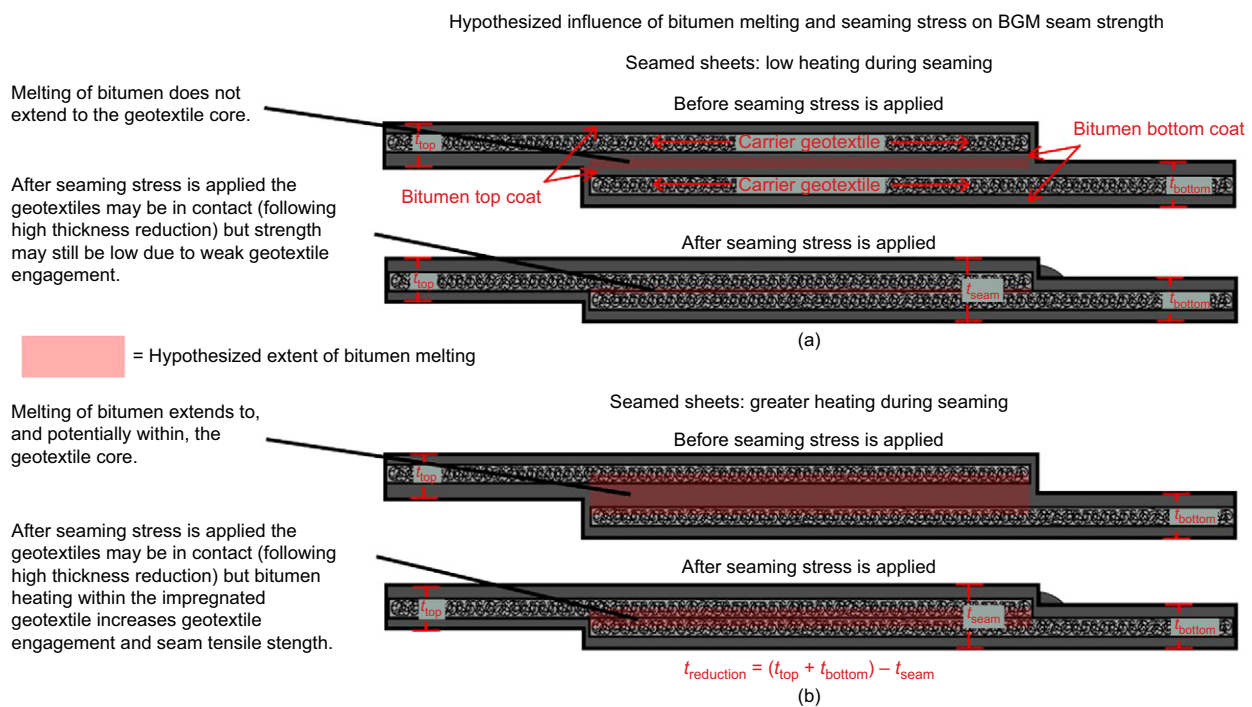
4.2. Creep rupture of geotextiles

The strength of the BGM sheet material is provided by the nonwoven geotextile core. Thus, the constant load rupture time of a BGM sheet is hypothesized to behave similarly to that of its nonwoven geotextile core. The BGM material examined contained a nonwoven polyester geotextile with a mass per unit area of 235 g/m^2 and a 50 g/m^2 glass fiber film. Bueno *et al.* (2005) reported the creep rupture times of a nonwoven polypropylene (PP) geotextile (mass per unit area 305 g/m^2) and a nonwoven polyester (PET) geotextile (mass per unit area 336 g/m^2), with the time until creep rupture under a load of 65% T_{ult} estimated as 12 years and 120 years for the PP and PET geotextiles, respectively. This is many orders of magnitude greater than those of the BGM seams examined, with both 0.1 mm and 0.4 mm thickness reduction seams exhibiting rupture times of less than one day for loads $\geq$45.9% T_{ult}.

4.3. Interactions at the seam

The application of pressure to heated bitumen within the seam overlap can be expected to mix the bitumen from the two BGMs to provide, following cooling, a solidified continuous layer engaging a portion of the geotextile fibers in each core. The greater the heat and pressure, the greater the squeeze-out and thickness reduction.

A conceptual view of the hypothesized interaction between the seam's bitumen component and its geotextile fibers is shown in Figure 5. High heating and seaming stress appear to increase both the melt depth of the bitumen within

Hypothesized influence of bitumen melting and seaming stress on BGM seam strength

Seamed sheets: low heating during seaming

Melting of bitumen does not extend to the geotextile core.

After seaming stress is applied the geotextiles may be in contact (following high thickness reduction) but strength may still be low due to weak geotextile engagement.

= Hypothesized extent of bitumen melting

Melting of bitumen extends to, and potentially within, the geotextile core.

After seaming stress is applied the geotextiles may be in contact (following high thickness reduction) but bitumen heating within the impregnated geotextile increases geotextile engagement and seam tensile stength.

Seamed sheets: greater heating during seaming

$t_{reduction} = (t_{top} + t_{bottom}) - t_{seam}$

Figure 5. Conceptual view of the hypothesized effect geotextile engagement has on seam tensile shear strength and constant tensile load failure time for (a) low heated seams, and (b) higher heated seams

the overlap and mix bitumen/remove air voids present within the overlap and geotextile core. Intimate contact between the bitumen matrix and the geotextile fibers post seaming engages the fibers in the geotextile, subsequently increasing tensile shear strength and constant tensile load failure time. Thus, with low heating and low stress (e.g. for hand-torch seams 5 kPa static load in Table 1), the bitumen melting only extended into the BGMs respective top and bottom bitumen coats (i.e. only the bitumen within the seam interface was heated and mixed following the application of seaming stress) and none of the bitumen near the geotextile was affected by the seaming process. The consequent lack of geotextile engagement produced seams with poor strength even with 200 mm overlap. In low heating and high stress cases (e.g. for hand-torch seams, hand roller: high in Table 1), bitumen melting still only extended into the BGMs' respective top and bottom bitumen coats but the higher seaming stress forced the geotextile cores into close proximity and removed air voids within the interface, subsequently increasing tensile strength for a given overlap. However, despite the high stress, the failure to melt the bitumen through to the core with a hand torch did not provide the same level of interaction between the fibers in the two cores as in the high heat (field torch and field roller; Table 1) cases, where good interaction was achieved even with low thickness reduction. This was likely responsible for the adequate tensile strength for the low overlap seams in Table 1. Based on this data and conceptual model, it is recommended that BGM seams and patches be created using the manufacturer specified field-torch in order to achieve effective heating through to the core.

Following greater heating time and/or increased seaming stress, field-torch seams with a high degree of thickness reduction and squeeze-out loss (i.e. ≥ 0.6 mm and 20–55 mm, respectively) are thought to have experienced excessive bitumen loss in the form of squeeze-out, subsequently reducing seam constant tensile load performance as there is less of a bitumen matrix to engage the geotextile core. Thus, seams with excessive squeeze-out loss may exhibit slightly lower time until failure than seams with the recommended 6 mm squeeze-out amount. This suggests that the bitumen component within the seam post-seaming provides tensile strength, and that too much loss of bitumen is deleterious regarding seam performance. Moreover, this suggests that geotextile heat tacking is likely not the primary factor providing strength to the BGM seam as one would suspect seam performance to remain essentially equal between the 6–10 mm and 20–55 mm squeeze-out seams if heat tacking of the geotextile, rather than bitumen interaction with the geotextile, was the primary component providing tensile strength. Conversely, if the geotextile fibers did not provide tensile strength, and only the bitumen component did, then one would expect low thickness reduction and squeeze-out seams (≤ 0.2 mm and 0 mm, respectively) to exhibit longer failure times than seams with greater thickness reduction and squeeze-out amount.

4.4. Practical applications

BGM seams should be assessed based on both immediate short-term strength and likely long-term strength. This includes tensile shear testing and an assessment of geotextile engagement following measurement of thickness reduction or seam squeeze-out, in conjunction with ultrasonic testing and vacuum box testing whenever possible. Air lance testing of BGM seams may also serve as a means of identifying discontinuities within the seam. However, due to the high unit weight of the BGM material, it is suspected that identification of discontinuities via this method may be more difficult for BGMs than for other GMB materials that commonly employ this CQA technique (e.g. polyvinyl chloride GMBs) (Scheirs 2009).

Prior to production seaming, a qualification seam should be conducted to ensure seaming practices meet or exceed the 0.8 weld factor and break location criteria, with the same pass/fail criteria based on seam strength and break locations applied to any subsequent destructive samples taken. Seam thickness reduction should be monitored for both qualification and destructive testing seams, and appropriate changes made to welding practices to attempt to attain average thickness reductions 0.2 mm $< t_r < 0.6$ mm and squeeze-out beads ≥ 6 mm whenever possible. When a seam's long-term integrity is in question, following the absence of squeeze-out and/or a low thickness reduction over an extended length of seam, it is suggested that a constant load tensile test be performed to assess the degree of geotextile engagement. This test can be conducted at loads of $\sim 55\%$ material ultimate strength and possibly higher. The chosen load for this test would be considered suitable as long as seam separation has occurred, and the exposed failure surface morphology of the seam can be examined. At higher loads, sheet failure may occur before shearing of the bitumen layer within the seam can occur. Thus, constant tensile loads for the assessment of geotextile engagement should be selected such that seam separation occurs in the shortest time manageable to accelerate testing. Ideally both the upper and lower sheet should have, to some degree, a rough exposed geotextile surface and fibers orientated in the direction of the applied load following rupture. The aforementioned tests suggest geotextile engagement within the seam may lead to an order of magnitude increase in the time until rupture of BGM seam subjected to constant tensile loads. If no evidence of geotextile engagement is observed, then appropriate measures, such as repairs, should be conducted. Furthermore, the absence of geotextile engagement may provide insight from a failure forensics perspective, where the failure surfaces of ruptured BGM seams can be examined to assess the effect geotextile engagement (or lack thereof) had on seam rupture.

The result presented herein suggests that BGM seams are susceptible to sustained tensile loads in the long term, and thus, that engineers should limit the extent of loading perpendicular to the seam direction when designing with BGMs. Care should be taken to avoid placing, whenever possible, BGM seams in areas suspected to experience significant displacement perpendicular to the seam direction, such as adjacent and parallel to joints on rigid structures, horizontally on side slopes, or where they could be significant differential settlement below a seam with an overlying cover soil.

5. CONCLUSIONS

This study examined the tensile shear strength and constant tensile load failure times of BGM seams created from one 4 mm BGM product. Seams were created using two different seaming techniques and were subjected to different seaming stresses and degrees of heating to produce seams with varying thickness reduction and squeeze-out amounts. The results show that the BGM seams tested were susceptible to a time-dependent failure when subjected to sustained tensile stress. Seam thickness reductions and the amount of squeeze-out were also found to serve as an indication of increased geotextile engagement for the seams tested. The following conclusions were reached for the specific BGM, welding equipment, and conditions examined:

(*a*) Following normal and lower heat applied welding practices, a seam weld factor of 0.8 is a reasonable lower limit for accepting BGM seams based on short-term performance.

(*b*) Failure surfaces of constant tensile load tested BGM seams suggest that lack of geotextile engagement played an important role in the failure times of BGM seams subjected to constant tensile stress.

(*c*) 200 mm overlap seams, for a 4 mm nominal thickness BGM, should have an average thickness reduction of ~0.4 mm with a ≥6 mm squeeze out bead to increase the likelihood of geotextile engagement occurring within the seam and higher constant tensile load failure times.

(*d*) Decreased thickness reduction and the absence of a seam squeeze-out bead resulted in an order of magnitude decrease in seam failure time when compared to seams with higher thickness reduction and an ~6 mm squeeze-out bead for the constant tensile loads examined.

(*e*) Just as tensile strains should be minimized in HDPE geomembranes, similarly it is important to minimize tensile stresses in BGMs, particularly near the location of seams in both cases.

(*f*) Although there is uncertainty associated with extrapolation, preliminary estimates based on the work presented in this paper suggest that, to get a service life of 50 and 100 years, the sustained tensile stress needs to be less than 3% and 2.6% the ultimate tensile strength of the sheet at 21°C, respectively (and possibly less at higher temperatures).

The conclusions given above are strongly supported by the data for the BGM and conditions examined. However, it is acknowledged that this paper only examined the constant tensile load failure times of BGM seams with 200 mm overlap subjected to loads between 18% and 55% of the sheet material strength at one reference temperature (21°C) for one BGM product. There is scope for significant future research into the effects on failure time and break characteristics of seams with lower loads, different overlap widths, different products and material thicknesses, and higher test temperatures. However, this work does serve as a warning that designers should consider the sensitivity of the project to seam failure if the seams can be subjected to sustained tension and that they should do constant load seam tests at realistic field temperatures (temperatures higher than the 21°C considered in the paper have the potential to accelerate failure) to verify suitability of the BGM seam for their project as part of their design process.

DATA AVAILABILITY STATEMENT

Some or all data, models, or code generated or used during the study are available from the corresponding author by request.

ACKNOWLEDGEMENTS

ABBREVIATIONS

BGM	bituminous geomembrane
CQA	construction quality assurance
GMB	geomembrane
HDPE	high density polyethylene
XD	cross-machine direction

REFERENCES

Addis, P., Andruchow, B. & Wislesky, L. (2013). Bituminous geomembrane failure as a co-disposal tailings storage facility. *Proc. Tailings and Mine Waste*, Banff, AB, Canada.

ASTM D5262-07. *Standard Test Method for Determining the Unconfined Tension Creep and Creep Rupture Behavior of Planar Geosynthetics Used for Reinforcement Purposes*. ASTM International, West Conshohocken, PA, USA.

ASTM D7056-07. *Standard Test Method for Determining the Tensile Shear Strength of Prefabricated Bituminous Geomembrane Seams*. ASTM International, West Conshohocken, PA, USA.

ASTM D7275-07. *Standard Test Method for Tensile Properties of Bituminous Geomembranes (BGMs)*. ASTM International, West Conshohocken, PA, USA.

Breul, B., Huru, M. & Palolahti, A. (2008). Use of bituminous geomembrane (BGM) liner for agnico eagle mine in Kittila (Finland). *Proc. of the 4th European Geosynthics Conference*, Edinburgh, Scotland, p. 245.

Bueno, B. D. S., Costanzi, M. & Zornberg, J. (2005). Conventional and accelerated creep tests on nonwoven needle-punched geotextiles. *Geosynthetics International*, **12**, No. 6, 276–287.

Clinton, M. & Rowe, R. K. (2017). Physical performance of a bituminous geomembrane for use as a basal liner in heap leach pads. *Proc., 70th Can. Geotech. Conf.*, Ottawa, Canada.

Cunning, J., Isidoro, A., Eldridge, T. & Reinson, J. (2008). Dam construction at Diavik using bituminous geomembrane liners. *Proceedings of the 61st Canadian Geotechnical Conference*, Edmonton, AB, Canada, pp. 21–24.

Daly, N., Aguirre, T., Breul, B. & Breul, B. & Barfett, B. (2018). Bituminous geomembranes (BGM) for heap leach pads and dumps

for solid wastes in mine construction. *Proceedings of the 71st Canadian Geotechnical Conference*, Edmonton, AB, Canada.

Francey, W. & Rowe, R. K. (2022). Long-term stress crack resistance of HDPE fusion seams aged at 85°C in synthetic leachate. *Canadian Geotechnical Journal*, **60**, No. 3, 251–268.

Francey, W. & Rowe, R. K. (2023a). Importance of thickness reduction and squeeze-out Std-OIT loss for HDPE geomembrane fusion seams. *Geotextiles and Geomembranes*, **51**, No. 2, 30–42, https://doi.org/10.1016/j.geotexmem.2022.09.003.

Francey, W. & Rowe, R. K. (2023b). Stress crack resistance of unaged high-density polyethylene geomembrane fusion seams. *Geosynthetics International*, **30**, No. 2, 154–168, https://doi.org/10.1680/jgein.21.00027a.

Gourc, J. & Delmas, P. (2016). The behaviour of 'alive' earthworks with geosynthetics after several decades. *Proc., 6th European Geosynthetics Conference*, Ljubljana, Slovenia, pp. 65–107.

Kavazanjian, E., Andresen, J. & Gutierrez, A. (2017). Experimental evaluation of HDPE geomembrane seam strain concentrations. *Geosynthetics International*, **24**, No. 4, 333–342.

Mafra, J., Mello, J., Eldridge, T. & Breul, B. (2008). Two case histories of dams waterproofing with bituminous geomembranes. *1st PanAm Geosyn. Conf.*, Cancun, Mexico.

Peggs, I. (2008). Prefabricated bituminous geomembrane: a candidate for exposed geomembrane caps for landfill closures. *1st PanAm Geosyn. Conf.*, Cancun, Mexico, pp. 191–197.

Rowe, R. K. & Francey, W. (2018). Effect of dual track wedge welding at 30°C ambient temperature on post-weld geomembrane oxidative induction time. *11ICG*, Seoul, Korea.

Rowe, R. K. & Shoaib, M. (2017). Long-term performance HDPE geomembrane seams in MSW leachate. *Canadian Geotechnical Journal*, **54**, No. 12, 1623–1636, https://doi.org/10.1139/cgj-2017-0049.

Rowe, R. K. & Shoaib, M. (2018). Durability of HDPE geomembrane seams immersed in brine for three years. *ASCE Journal of Geotechnical and Geoenvironmental Engineering*, **144**, No. 2, https://doi.org/10.1061/(ASCE)GT.1943-5606.0001817.

Samea, A. & Abdelaal, F. B. (2023). Effect of elevated temperatures on the degradation behaviour of elastomeric bituminous geomembranes. *Geotextiles and Geomembranes*, **51**, No. 1, 219–232.

Scheirs, J. (2009). *A Guide to Polymeric Geomembranes: a Practical Approach*. John Wiley & Sons, West Sussex, UK.

Touze-Foltz, N. & Farcas, F. (2017). Long-term performance and binder chemical structure evolution of elastomeric bituminous geomembranes. *Geotextiles and Geomembranes*, **45**, No. 2, 121–130.

Turley, M. & Gautier, J. (2004). Twenty five years experience using bituminous geomembranes as upstream waterproofing for structures. *Proc., Long-term Benefits and Performance of Dams: Proc. 13th Con.*, British Dam Society, Canterbury, UK, pp. 94–101.

Zhang, L., Bouazza, A., Rowe, R. & Scheirs, J. (2017). Effect of welding parameters on properties of HDPE geomembrane seams. *Geosynthetics International*, **24**, No. 4, 408–418.

The Editor welcomes discussion on all papers published in Geosynthetics International. Please email your contribution to discussion@geosynthetics-international.com